Laser imprint reduction with a short shaping laser pulse incident upon a foam-plastic target

Nathan Metzler

Science Applications International Corporation, McLean, VA 22150, and

Physics Department, Nuclear Research Center Negev, P. O. Box 9001, Beer Sheva, Israel

Alexander L. Velikovich and Andrew J. Schmitt

Plasma Physics Division, Naval Research Laboratory, Washington, D.C. 20375

John H. Gardner

LCP&FD, Naval Research Laboratory, Washington, D.C. 20375

Abstract

In the previous work [Metzler *et al*., Phys. Plasmas **6**, 3283 (1999)] it was shown that a tailored density profile could be very effective in smoothing out the laser beam non-uniformities imprinted into a laser-accelerated target. However, a target with a smoothly graded density is difficult to manufacture. A method of dynamically producing a graded density profile with a short shaping laser pulse irradiating a foam layer on top of the payload prior to the drive pulse is proposed. It is demonstrated that the intensity and the duration of the shaping pulse, the time interval between the shaping pulse and the drive pulse, and the density ratio between the foam and the payload can be selected so that the laser imprint of the drive pulse is considerably suppressed without increasing the entropy of the payload. The use of the foam-plastic target *and* a shaping pulse reduces the imprinted mass perturbation amplitude by more than an order of magnitude compared to a solid plastic target. The requirements to the smoothing of the drive and shaping laser beams and to the surface finish of the foam-plastic sandwich target are discussed.

PACS numbers: 52.57.Fg, 52.57.-z

Report Documentation Page

Form Approved
OMB No. 0704-0188

1. REPORT DATE	2. REPORT TYPE	3. DATES COVERED
2002		**00-00-2002 to 00-00-2002**

4. TITLE AND SUBTITLE	5a. CONTRACT NUMBER
Laser imprint reduction with a short shaping laser pulse incident upon a foam-plastic target	5b. GRANT NUMBER
	5c. PROGRAM ELEMENT NUMBER
6. AUTHOR(S)	5d. PROJECT NUMBER
	5e. TASK NUMBER
	5f. WORK UNIT NUMBER
7. PERFORMING ORGANIZATION NAME(S) AND ADDRESS(ES) **Naval Research Laboratory,Plasma Physics Division,4555 Overlook Avenue SW,Washington,DC,20375**	8. PERFORMING ORGANIZATION REPORT NUMBER
9. SPONSORING/MONITORING AGENCY NAME(S) AND ADDRESS(ES)	10. SPONSOR/MONITOR'S ACRONYM(S)
	11. SPONSOR/MONITOR'S REPORT NUMBER(S)

12. DISTRIBUTION/AVAILABILITY STATEMENT
Approved for public release; distribution unlimited

13. SUPPLEMENTARY NOTES
This article appears in the December 2002 issue of Physics of Plasmas and can be found at Phys. Plasmas 9(12), 5050 (2002)

14. ABSTRACT
In the previous work [Metzler et al., Phys. Plasmas 6, 3283 (1999)] it was shown that a tailored density profile could be very effective in smoothing out the laser beam non-uniformities imprinted into a laser-accelerated target. However, a target with a smoothly graded density is difficult to manufacture. A method of dynamically producing a graded density profile with a short shaping laser pulse irradiating a foam layer on top of the payload prior to the drive pulse is proposed. It is demonstrated that the intensity and the duration of the shaping pulse, the time interval between the shaping pulse and the drive pulse, and the density ratio between the foam and the payload can be selected so that the laser imprint of the drive pulse is considerably suppressed without increasing the entropy of the payload. The use of the foam-plastic target and a shaping pulse reduces the imprinted mass perturbation amplitude by more than an order of magnitude compared to a solid plastic target. The requirements to the smoothing of the drive and shaping laser beams and to the surface finish of the foam-plastic sandwich target are discussed.

15. SUBJECT TERMS

16. SECURITY CLASSIFICATION OF:			17. LIMITATION OF ABSTRACT	18. NUMBER OF PAGES	19a. NAME OF RESPONSIBLE PERSON
a. REPORT	b. ABSTRACT	c. THIS PAGE			
unclassified	**unclassified**	**unclassified**	**Same as Report (SAR)**	**37**	

I. INTRODUCTION.

Reduction of the laser imprint remains one of the important problems of the direct-drive laser fusion. Even with all the improvements of the optical smoothing techniques, the residual laser beam non-uniformities imprinted into the imploding target could be amplified by the Rayleigh-Taylor (RT) instability to amplitudes large enough to prevent high gain or even ignition.[1,2]

Most approaches to making advanced imprint-resistant targets investigated so far are based on using either low-density foam layers;[3, 4] external x rays for creating a plasma before the drive laser pulse,[5, 6] or x rays from high-Z materials in the target itself heated by the laser beam used to drive the target,[2] or some hybrid combinations (such as foams preheated by x rays[4, 6-10] or a high-Z layer on the plastic membrane of cryogenic deuterium-loaded-foam targets[11]). The hybrid approach [4, 6-10] uses x rays early in the pulse to pre-heat the outer layers of the target, while most of the target mass is maintained on the low adiabat. Alternatively, a short laser pre-pulse before the arrival of the drive pulse could be used for pre-heating.[12-15] The purpose of pre-heating in all these cases is to decrease the density and to increase the temperature of the outer layers of the target some time before the drive laser pulse arrives. Both factors reduce the RT growth rate: the lower density contributes by increasing the mass ablation velocity, whereas the higher temperature increases the smoothing due to thermal conductivity. The pre-heating must be confined to the outer layers of the target so that the imploded fuel remains on a low adiabat consistent with ignition or high gain. One should also mention a related early idea of replacing a single shaped laser pulse with a train of shorter pulses to improve the

target performance[16] (the concept that has recently re-emerged as the picket fence approach to shaping the low-intensity foot of the laser pulse[17]).

A different approach to the mitigation of laser imprint is the use of tailored density profiles, first suggested in Ref. 3. The method of density tailoring was originally proposed to mitigate the RT instability in Z-pinch implosions.[18] The stabilizing effect is obtained by shock waves slowing down as they propagate into increasing density. The effective gravity near the shock front then has the same direction as the density gradient, which makes the mass perturbations in the shocked plasma oscillate rather than grow. Density tailoring seems to improve radiative performance of Z-pinch plasma radiation sources: For example, the cross-section of the gas jet formed by a double-shell nozzle[19] (which corresponded to an appropriately tailored radial density profile) was shown to give the most significant contribution to the record-high argon K-shell yield (270 kJ) recently obtained on the Z facility in Sandia. [20]

Even if the laser target initially has no density gradient, the mass variation amplitude will oscillate during the shock transit, as predicted by theory[21] and simulations,[22] and recently confirmed by experiments on the Nike laser at the Naval Research Laboratory (NRL).[23,24] The additional effective gravity provided by the density tailoring helps increase the frequency and reduce the amplitude of such oscillations, which results in a very efficient suppression of the laser imprint. Simulations of Ref. 3 demonstrated that a planar target with a tailored density profile is much more imprint-resistant than either a low-density target or a foam-plastic sandwich target of the same total mass and thickness. There is some experimental evidence[25] that a target approximating a graded profile with a three-stepped density structure (layers of foam

with densities 0.04, 0.12, 0.37 g/cm^3, each 5 μm thick) was more imprint-resistant in a wide range of wavelengths than a single slab of a low-density foam.

At the moment, no technology is available to manufacture a foam target whose density is smoothly graded in one (radial) direction. However, the same physical mechanism of laser imprint mitigation through inverted acceleration [3] could be used if the tailored density profile were produced on the fly dynamically; by a separate short laser pulse incident upon the appropriately designed target prior to the drive laser pulse. Such a target might consist of a sandwich of a low-density foam on top of a higher-density payload. We will call this short pulse a shaping pulse to emphasize its purpose (shaping the density profile), differentiating it from a pre-pulse[12-14] or a high-intensity spike, a picket at the start of the foot preceding the main drive pulse.[15] The shock wave(s) launched by the drive laser pulse then propagate(s) through the graded density profile created by the expansion wave which follows the first shock wave produced by the shaping pulse. The intensity and the duration of the shaping pulse, the time interval between the shaping pulse and the drive pulse, and the density ratio between the foam and the payload can be selected self-consistently to provide a shock impedance matching between the foam and the payload. The shock waves generated by the shaping pulse and the drive pulse are timed to merge when they reach the contact interface between the shock-compressed foam and the payload, and there is no shock reflection from this interface because the density of the shock-compressed foam is close to the density of the payload. It should be noted that the purpose of the shaping laser pulse needed for this method is different from that discussed in previous works. [12-17] Our goal is not primarily to pre-heat and soften the outer layers of the target. Rather, we intend to dynamically

generate a tailored density profile that satisfies the conditions of shock impedance matching. This requires a more complex design — in particular, the outer foam layer must be appropriately designed to produce the tailored density profile. This design, however, leads to a much higher efficiency of imprint mitigation compared to that achieved by pre-heating the outer layers of a solid target. [12-15]

This paper is structured as follows. In Section II we describe how the shaping pulse and the target parameters are chosen to produce the desired tailored density profile, achieving at the same time the shock impedance matching at the foam/payload interface. In Section III we demonstrate that the target designed this way is imprint-resistant and find the limitations imposed on the non-uniformity of the smoothed shaping pulse and drive laser pulse beams, and on the target surface finish. In Section IV we conclude with a discussion.

II. TAILORING A DENSITY PROFILE WITH A SHAPING LASER PULSE

This Section investigates the tailoring of a density profile with a shaping laser pulse in a planar foam-plastic layer (sandwich) target for laser imprint mitigation. The goal is to find the conditions under which this concept could be experimentally tested in planar geometry, similar to earlier experiments.[2,21,22] The planar target emulates the early-time performance of a small part of a spherical target. This is adequate for modeling the imprint mitigation, since the perturbations imprinted into the accelerated plasma from the optically smoothed laser beam are mostly in the short wavelength range and the target moves only a small fraction of the radius. Nike experiments (laser wavelength $\lambda = 0.248$ μm, focal length $f = 600$ cm, diameter of the laser aperture $D_A = 15$

cm), are typically conducted with ISI smoothing at 1 THz bandwidth, which puts most of the laser imprint in the wavelength range 20-30 μm (see Ref. 26), whereas the flat central region of the Nike beam[27] is 400 μm in diameter compared to a typical ICF pellet radius of over a millimeter.

What is referred to as the drive laser pulse is the Nike pulse with or without a low-intensity foot, which sets the accelerated payload at the proper adiabat (for details, see Ref. 28). The energy of the shaping pulse is very small compared to the energy of the drive pulse.

The graded density profile is formed in a process called impulsive loading. This can be idealized as a fast release of a finite energy in a thin layer near the surface $x = 0$ of a half-space $x \le 0$ filled with a uniform material at rest.[29] Impulsive loading has been studied since the 1950s when it was visualized as an explosion of a thin layer of explosive on a surface, or an impact of a thin, light plate carrying a finite kinetic energy. A short-duration shaping laser pulse delivering a finite energy to a thin surface layer of the foam also acts as an impulsive load. The impulsive loading produces a shock wave that propagates into the target in the negative x direction, and is immediately followed by an expansion wave which gradually reduces the shock strength, accelerating the fluid in the positive x direction. If the shock wave is sufficiently strong, and the ideal gas model is a good approximation of the equation of state, then the flow of the shocked fluid is self-similar.[29,30] The position of the shock front at time t is given by

$$x_s(t) = -\xi_0 \left(\frac{I_p}{\rho_0} \right)^{1/3} \tau^{1-\alpha} t^{\alpha} = -\xi_0 \left(\frac{E_p}{\rho_0} \right)^{1/3} \tau^{2/3-\alpha} t^{\alpha}, \qquad (1)$$

where I_p and τ are the intensity and duration of the shaping pulse, respectively, $E_p = I_p \tau$ is the energy per unit area delivered in the impulsive loading, α is the self-similarity exponent, ξ_0 is the dimensionless factor depending on the equation of state. The scaling of $x_s(t)$ with E_p and ρ_0 is the same as in the case of a planar blast wave.[31] In the latter case, the dependence of $x_s(t)$ on all the relevant parameters is obtained directly from the dimensional considerations:

$$x_s(t) = -\tilde{\xi}_0 \left(\frac{E_p}{\rho_0} \right)^{1/3} t^{2/3}, \tag{2}$$

where the constant $\tilde{\xi}_0$ corresponding to the blast wave solution of Ref. 31, is, of course, different from ξ_0 in (1). Proportionality between $x_s(t)$ and $(E_p / \rho_0)^{1/3}$ in (1), of course, follows from the same dimensional considerations. The time dependence in (1), however, cannot be found this way, since the self-similar solution under consideration belongs to the so-called second kind.[29] The self-similarity exponent α is, in a general case, an irrational number determined from the condition of analyticity of the self-similar solution on the limiting characteristic. Note that the shock motion in the limit $\tau \to 0$, $I_p \to \infty$, finite E_p, is not determined by the energy E_p instantly released, as is the case for the blast wave (2), but rather by some combination of E_p and τ. Obviously, α must be less than one, so that the shock wave slows down as it propagates. A more detailed analysis in Ref. 30 yields the following inequalities for α:

$$\frac{1}{2} < \alpha < \frac{2}{3}. \tag{3}$$

Comparing (1) and (2), we see why α should not exceed 2/3: this value of the self-similarity exponent corresponds to the case of a blast wave, where the shocked fluid does not expand beyond the plane of symmetry, $x = 0$, whereas our case of impulsive loading permits unlimited expansion in the positive x direction.[29] Therefore the blast wave is supported by a higher pressure, and accordingly, its asymptotic decay is slower.

The self-similar density profile is expressed as

$$\rho(x,t) = \begin{cases} \rho_0, & x < x_s(t); \\ \dfrac{\gamma+1}{\gamma-1}\rho_0 N(\eta), & x \geq x_s(t), \end{cases} \tag{4}$$

where

$$\eta = \frac{x}{x_s(t)}. \tag{5}$$

is the self-similar coordinate, and the function $N(\eta)$ satisfying $N(1) = 1$ determines the shape of the profile. The time dependence of the self-similar profile is thus reduced by its stretching along the horizontal axis. The density peaks near the shock front and decays with increased distance from it, asymptotically as $N(\eta) \sim |\eta|^{-1/(1-\alpha)}$ at $\eta \to -\infty$. There is an exceptional case of $\gamma = 7/5$, for which the self-similar solution is found explicitly:[30]

$$\alpha = 3/5, \qquad N(\eta) = (5-4\eta)^{-5/2}, \qquad -\infty < \eta \leq 1. \tag{6}$$

The dynamically formed density profile (4) satisfies the requirements of Ref. 3 to provide an efficient imprint stabilization. Of course, the impulsive loading is not fully equivalent to manufacturing a target with a graded density, since the fluid pressure and velocity are nonzero now, also featuring the self-similar profiles. However, the shock wave launched by drive laser pulse will be much stronger than one generated by the shaping pulse. Therefore, the pressure and velocity variation in front of this strong shock

wave are of minor importance, and its propagation is governed mostly by the pressure driving it and the density profile ahead of its front, just as in Ref. 3. In particular, the shock generated by the drive pulse sets the payload at almost the same adiabat as it would without the shaping pulse.

To provide the approximate shock impedance matching, the peak density in the graded profile, $(\gamma+1)\rho_0/(\gamma-1)$, must be equal to the density of the payload, ρ_1, i. e.

$$\rho_0 \cong \frac{\gamma-1}{\gamma+1}\rho_1 . \tag{7}$$

The density tailoring can only help stabilize the wavelengths that are not much longer than the thickness of the graded density layer. The initial foam layer is shock-compressed approximately by a factor of $(\gamma+1)/(\gamma-1)$, hence its initial thickness L_0 is chosen from the condition

$$L_0 \cong \frac{\gamma+1}{\gamma-1}\lambda_m , \tag{8}$$

where $\lambda = \lambda_m$ is the longest wavelength to be stabilized. For instance, assuming that the payload is made of a solid plastic, $\rho_1 = 1.07$ g/cm,^{3} $\lambda_m = 30$ μm as above, and $\gamma = 5/3$ for a plastic foam, we find the approximate parameters of the foam layer: $\rho_0 = 0.27$ g/cm^3, $L_0 = 120$ μm. The time interval between the shaping pulse and the drive laser pulse should be found from the requirement that the two shock waves merge when they hit the payload.

Our numerical simulations were made with the FAST2D hydrocode developed at NRL[32] (more details about the code and further references are given in Refs. 1, 3). We ran the code in a 1-D mode in order to verify the above theoretical considerations and to

do the matching. Figure 1 shows the density profiles resulting from the irradiation of a 120 μm thick CH foam layer ($\rho_0 = 0.39$ g/cm^3) with a $\tau = 0.325$ ns long shaping pulse at laser wavelength $\lambda_L = 0.248$ μm and intensity $I_p = 4.1$ TW/cm^2, delivering the energy $E_p = 1.33$ kJ/cm^2. Propagation of the shock wave shown in Fig. 1 is well approximated by the expression (1) with $\alpha = 0.685$ and $\xi_0 = 0.604$, which can be re-written as

$$x_s(t) = -13 \times \left(\frac{E_p, \text{kJ/cm}^2}{\rho_0, \text{g/cm}^3} \right)^{1/3} \times (\tau, \text{ns})^{-0.0183} \times (t, \text{ns})^{0.685} \ \text{μm} . \qquad (9)$$

Having varied E_p and ρ_0, and we have checked that Eq. (9) is indeed a good wide-range approximation for a CH foam impulsively loaded with a short laser pulse. Note that the self-similarity exponent α is outside of the range in Eq. (3), although fairly close to its upper boundary, which indicates that the shock dynamics is mainly determined by the laser energy deposited at the surface, and is almost independent of the pulse duration. The small deviation from (3) is not surprising, since the simulation deals with approximate rather than exact self-similarity of the flow: the equation of state is realistic, not an ideal gas model, and the shock compression gradually decreases as the shock wave slows down; see Fig. 1. Of course, a planar blast wave launched by deposition of the same energy per unit area would propagate faster, at the times of interest, primarily due to a larger value of the coefficient $\tilde{\xi}_0$. We have checked this by making the plasma bounded by a rigid wall at $x = 0$, and found that the shock trajectory is well approximated by the formula like (9) with no dependence on τ, the appropriate power $\alpha = 2/3$ and the coefficient about 30 instead of 13, in agreement with the blast wave solution (2) of Ref.

31. Deviation from the exact self-similarity, particularly the gradual reduction of shock strength and density compression ratio, is the reason why we chose a somewhat higher foam density than that given by (8), in order to ensure the shock impedance matching after the first shock wave travels 120 μm.

Figure 2 shows the shock dynamics for the case when the above shaping pulse is followed by the drive pulse after $\Delta t \cong 12$ ns (the interval between the shaping pulse and the drive pulse reaching half-maximum). For the drive laser pulse, we have taken a 4-ns long Nike pulse[27] without a foot [Fig. 3(a), dashed line]. The density profiles [Fig. 2(a)] and the *x*-*t* diagram [Fig. 2(b)] demonstrate a good matching, both in time (the two shock waves merge when they hit the interface between the foam layer and the payload) and in shock impedance (no shock reflection is observed). In the next section we will demonstrate that the density profile has the desired properties needed to reduce the laser imprint.

Fig. 3(a) shows the shape of the Nike pulse and Fig. 3(b) - the corresponding *x*-*t* diagrams for a 62-μm solid plastic target. For this case we used the Nike pulse shape with a foot to control the target adiabat. We see that the ablation front in Fig. 3(b) is never concave, which corresponds to its acceleration (in the negative *x*-direction). In contrast with this, the ablation front shown in Fig. 2(b) is visibly concave before any shock reaches the payload, thus indicating effective deceleration, which makes the areal mass perturbations oscillate rather than grow. Thus, the imprint is inhibited *before the target acceleration starts*, in a similar manner as in graded density targets.[3] Simulations reported in the next Section confirm this statement.

III. STABILIZING EFFECT OF A DYNAMICALLY TAILORED DENSITY PROFILE

This Section investigates the efficiency of the density profile shaping described above for laser imprint mitigation. We now use the the FAST2D hydrocode in a 2-D mode. The radiation package of FAST2D has not been invoked in the simulations reported here. In our previous modeling[3,33] we have verified that radiation has only a small effect on the acceleration of planar plastic targets. To quantify the stabilizing effect of density tailoring with a shaping laser pulse, one needs some reference points for comparison. As first shown theoretically[3] and then confirmed experimentally,[25] the structure of the sandwich plastic-foam target (see Ref. 3, target 2, and Fig. 4 therein) is already much more imprint-resistant than a uniform solid target. All the targets are accelerated with a 4-ns Nike pulse[27] preceded by a ~3-ns low-intensity foot: $\lambda_L = 0.248$ μm, with peak intensity 50 TW/cm^2, time $t = 0$ corresponds to the instant when the laser intensity reaches half maximum. Duration of the laser shaping pulse is varied from 0.325 ns to 1.3 ns, while the energy delivered by the shaping pulse to the target is kept constant, 1.33 kJ/cm^2.

Figure 4(a) compares the perturbation growth in a sandwich target with and without the shaping pulse, and in a solid plastic target. Figure 4(b) compares the results for a 0.325-ns, a 1.3-ns, and a 0.1 ns shaping pulse. The areal mass variation amplitude in Fig. 4(a) is normalized to the solid plastic density, 1.07 g/cm^3, and thus expressed in microns (not to be confused with the amplitude of interfacial ripples, see discussion in Ref. 24 for details). For the simulations in Fig. 4 the laser nonuniformity is modeled as a 0.2% single-mode, constant-phase sine-wave intensity perturbation at $\lambda = 30$ μm superimposed on an otherwise spatially uniform drive laser pulse. The intensity perturbation in the shaping pulse is introduced in a similar way, and the curves in Fig.

4(a) show the effect of varying the shaping pulse perturbation amplitude from 0 to 0.2% to 2%. Figure 4(a) also presents the corresponding time histories obtained with the same drive pulse (but without any shaping pulse), for the same plastic-foam sandwich target and for a 62-μm solid plastic target.

The solid plastic target is strongly distorted by the drive pulse. If the drive pulse lasted any longer, a bubble would have punctured through the target. The foam-plastic sandwich target without the shaping pulse is somewhat less distorted. However, the areal mass oscillations produced by the drive pulse[3] are so strong that this target — with a relative mass variation slightly below 20% - is not likely to survive much more acceleration. A shaping pulse with a 2% intensity variation brings a considerable improvement — by a factor of 2-3. Not unexpectedlythe best results are found for the 0.2% and 0% intensity variation in the shaping pulse. Surprisingly, the mass variation amplitude in the case of a 0.2% is even less than it would be with a perfectly smooth shaping pulse: 0%! The explanation is simple: with the intensity variation given by the same sine wave function for both the shaping pulse and the drive pulse, the hydrodynamic perturbations caused by these pulses are coherent, they can interfere, and in this case they are seen to interfere negatively.

Shorter shaping pulses in Fig. 4(b) provide better stabilization. This is explained by the properties of the mass perturbation growth caused by a single-mode laser intensity modulation during the shock transit time, which have been established in the studies of laser imprint.[22] Let us assume that the shaping pulse duration τ is shorter than the decoupling time t_{dc} between the critical surface and the ablation front: $t_{dc} > \tau$. This decoupling time is the characteristic smoothing time of the pressure modulation at the

ablation front caused by the laser intensity modulation in the absorption zone. The smoothing of pressure modulation is due to the buildup of the plasma corona separating the two regions, i. e. $t_{dc} \cong 1/kv_c$, where k is the perturbation wave number, and v_c is the velocity of the absorption zone with respect to the ablation front. Then the time dependence of the areal mass modulation amplitude could be presented as[22]

$$\delta m(t) = \frac{\rho_0}{k} \times \frac{\delta I_p}{I_p} \times F(kUt), \tag{10}$$

where $\delta I_p / I_p$ is the relative modulation amplitude of the shaping beam intensity, U is the mass velocity of the shocked plasma, $F(\tilde{t})$ is a function of normalized time $\tilde{t} = kUt$. For the sake of simplicity we neglect the weak parametric dependence of $F(\tilde{t})$ on the laser intensity via the blowoff-plasma-to-ablation-front density ratio. Then for the short times of interest, $F(\tilde{t})$ is simply a growing function of its dimensionless argument, approximately proportional to $\tilde{t}^2$. The mass velocity U scales as $p_a^{1/2}$, where p_a is the ablative pressure driving the shock wave, which, in turn, scales as some power of the intensity I_p of the shaping laser beam: $p_a \propto I_p^{\nu}$, with ν somewhere between 0.66 and 0.8. We compare the shaping pulses at constant energy E_p per unit area, $I_p = E_p / \tau \propto \tau^{-1}$, so that $U \propto \tau^{-\nu/2}$. The end of the shaping pulse $t = \tau$ thus corresponds to a dimensionless time $\tilde{t}_p = kU\tau \propto \tau^{1-\nu/2}$. Since $\nu/2 < 1$, Eq. (10) demonstrates that a shorter shaping pulse will cause smaller perturbation imprint into the flow at the end of the pulse $\delta m(t = \tau) \propto \tau^{2-\nu}$. Moreover, even the time derivative of the mass perturbation at the end of the shaping pulse is smaller for a shorter pulse. This conclusion does not change if we take into account the weak parametric dependence of $F(\tilde{t})$ on the laser

intensity via the density ratio and the decoupling of the intensity modulation in the shaping beam from the pressure perturbations at the ablation front. Both effects are more pronounced at higher laser intensities and tend to decrease the mass variation.

Realistically, a target cannot be manufactured perfectly smooth. Since the surface finish and the intensity variation in the beam are both relatively small and uncorrelated, their effects could be studied separately. Figure 5 demonstrates the perturbation growth caused by placing a single-mode ripple, $\lambda = 30\mu m$, peak-to-valley amplitude $2a_0 = 2$ μm on the foam surface (an areal mass modulation equivalent to 0.79 μm in solid CH), while the shaping pulse and the drive beam are held perfectly smooth. A 2 m perturbation is much worse than the surface finish expected for an ICF target. We observe that the perturbation with the laser shaping pulse grows to almost as large an amplitude as without it. In this case the shaping pulse is seen to cause strong sonic oscillations in the shocked plasma, which amplify the mass variation in the ripples by a factor of 3-4 and persist until the drive laser pulse arrives to provide a higher (in comparison with the original surface ripples) initial perturbation for the subsequent growth. This rather unexpected behavior is because the perturbed flow contains a rippled expansion wave, which immediately follows the rippled shock wave. Oscillations of a rippled shock wave are known to decay from their peak initial amplitude to the lower values, see[24] and references therein. On the contrary, some amplification — by a factor of three or so - of the initial mass variation amplitude is characteristic of a rippled rarefaction wave.[24,33] The large-amplitude oscillations seen in Fig. 5 after the shaping pulse are apparently caused by the expansion wave component of the flow. From our simulations we conclude that the rms surface finish at $\lambda = 30$ μm should not exceed 0.1 μm, which is consistent with

the conventional smoothness requirements for direct drive laser fusion targets. Note that no additional requirements are made for the rear (inner) surface roughness, as the shock wave driven by the drive laser pulse merges with that driven by the shaping pulse before it hits the rear surface.

Now consider the residual non-uniformity of both the shaping pulse and the drive laser pulse left with ISI smoothing. The theoretical model of this smoothing technique and its numerical implementation in FAST2D are described in detail in Ref. 26. We assume a bandwidth of 1 TW, which implies a rms intensity variation in a single Nike beam time-averaged over 4 ns of less than 2%. With N_B statistically independent overlapping beams, the intensity variation in wavelengths greater than 10 m decreases further by a factor of $N_B^{-1/2}$, to about 0.25% for Nike s $N_B \cong 36$. For the shaping pulse, which is shorter than 4 ns, the time-averaged rms intensity variation in a single beam is higher by a factor of $(4\,\mathrm{ns}/\tau)^{1/2} \sim 2$ to 3.5.

As far as the energy is concerned, one beam out of 36 (with a pulse shortened to 1 ns or less) would be sufficient to provide the desired energy of the shaping pulse, since the shaping pulse needs less than 1% of the laser energy in the drive pulse. However, a single beam is 6 times less uniform than 36 overlapping beams. The question is whether a single beam is sufficiently smooth not to pre-introduce the imprint before the drive pulse.

Figure 6 answers this question. It compares the cases where [Fig. 6(a)] the shaping pulse is delivered by a single beam, ISI-smoothed at 1 THz to cases [Fig. 6(b)] with 36 such beams, overlapped and carrying the same energy to the target. The drive laser beam in both cases consists of 36 beams. We see that a single beam used as a shaping pulse is definitely not smooth enough to mitigate the imprint. The single beam

imprints enough perturbations of its own, that the resulting mass variation amplitude is even larger than in the absence of a shaping pulse. On the other hand, with the shaping pulse sufficiently smoothed (that is, with the same number of beams as in the drive pulse), it obviously helps to mitigate the imprint caused by the non-uniformity in the drive pulse, Fig. 6(b). Reduction of the non-uniformity of a single laser beam by almost another order of magnitude through increased bandwidth is hardly practical, see Ref. 24. Therefore the shaping pulse should be formed by overlapping multiple optically smoothed laser beams.

III. CONCLUSIONS

We have demonstrated that the mass imprint can be reduced by use of a single shaping laser pulse, with the effect as large as is predicted for a tailored density profile.[3] The energy of the shaping pulse can be a small fraction, less than 1%, of the total energy in the drive laser beam. The shaping pulse must be short on the nanosecond time scale: 1 ns duration will do, 0.3 ns is better.

We found that the shaping pulse must also be smoothed sufficiently to mitigate the imprint. Otherwise, the shaping pulse imprints its own non-uniformity, which persists during the time interval between the shaping pulse and the drive pulse in the form of strong sonic waves, providing seeds for the perturbation growth associated with the drive pulse. Similarly, the shaping pulse can increase the initial surface roughness in the target, transforming this initial mass variation into strong sonic waves on the target surface. There is a corresponding upper limit on the surface finish of the target. The requirements on the smoothness of the shaping pulse and the target surface are strict, but not

unrealistic. In particular, the laser drive uniformity available with 36 overlapping Nike beams, ISI-smoothed at 1 THz, seems to be sufficient for this purpose.

High-gain or ignition direct-drive targets that use this method for mitigating the laser imprint could be designed, but this task is beyond the scope of the present paper. A necessary intermediate step is designing and performing an experiment to demonstrate in planar geometry the efficiency of this method of imprint mitigation. This work is now in progress. It is too early to extrapolate to large-scale facilities, and we limit ourselves to the following observation. Since the energy in the shaping pulse is less than 1% of the energy in the drive beam, our method of stabilization at the ignition energy level (~1 MJ in the drive pulse) would require something like a 36-beam, 10-kJ laser, somewhat more powerful than Nike but a lot less powerful, less expensive and less complicated than the ~100 kJ picosecond laser needed to pursue the fast ignition option.[34]

Acknowledgements

The authors are grateful to Y. Aglitskiy and S. P. Obenschain for stimulating discussions of the experimental capabilities available on Nike, and to S. E. Bodner and V. N. Goncharov for helpful discussion of the theoretical issues. One of us (N. M.) wishes to thank Dr. S. P. Obenschain and Laser Plasma Branch at NRL for their support and hospitality during the performance of this research. This work was sponsored by the U.S. Department of Energy through the contract for the Naval Research Laboratory.

References

[1] A. J. Schmitt, A. L. Velikovich, J. H. Gardner, C. Pawley, S. P. Obenschain, Y. Aglitskiy, Y. Chan, Phys. Plasmas **8**, 2287 (2001).

[2] S. P. Obenschain, D. G. Colombant, M. Karasik, C. J. Pawley, V. Serlin, A. J. Schmitt, J. L. Weaver, J. H. Gardner, L. Phillips, Y. Aglitskiy, Y. Chan, J. P. Dahlburg, and M. Klapisch, Phys. Plasmas **9**, 2234 (2002).

[3] N. Metzler, A. L. Velikovich, and J. H. Gardner, Phys. Plasmas **6**, 3283 (1999).

[4] H. Nishimura, H. Shiraga, M. Nishikino, N. Miyanaga, T. Norimatsu, K. Nagai, K. Fujita, M. Heya, Y. Ochi, M. Nishikino, N. Ohnishi, A. Sunahara, M. Nakai, H. Azechi, H. Takabe, T. Yamanaka, and K. Mima, Bull. Am. Phys. Soc. **43**, 1666 (1998).

[5] M. Desselberger, T. Afshar-rad, E. Khattak, S. Viana, and O. Willi, Phys. Rev. Lett. **68**, 1539 (1992).

[6] H. Nishimura, H. Shiraga, H. Azechi, N. Miyanaga, M. Nakai, N. Izumi, M. Nishikino, M. Heya, K. Fujita, Y. Ochi, K. Shigemori, N. Ohnishi, M. Murakami, K. Nishihara, R. Ishizaki, H. Takabe, K. Nagai, T. Norimatsu, M. Nakatsuka, T. Yamanaka, S. Nakai, C. Yamanaka, K. Mima, Nuclear Fusion **40**, 547 (2000).

[7] M. Desselberger, M. W. Jones, J. Edwards, M. Dunne, and O. Willi, Phys. Rev. Lett. **74**, 2961 (1995).

[8] R. G. Watt, J. Duke, C. J. Fontes, P. L. Gobby, R. V. Hollis, P. A. Kopp, R. J. Mason, and D. C. Wilson, Phys. Rev. Lett. **81**, 4644 (1998).

[9] M. Dunne, M. Borghesi, A. Iwase, M. W. Jones, R. Taylor, R. Gibson, S. R. Goldman, J. Mack, and R. G. Watt, Phys. Rev. Lett. **75**, 3858 (1995). [10]

[10] R. J. Mason, R. A. Kopp, H. X. Vu, D. C. Wilson DC, S. R. Goldman, R. G. Watt, M. Dunne, O. Willi, Phys. Plasmas **5**, 211 (1998).

[11] J. D. Sethian, S. E. Bodner, D. G. Colombant, J. P. Dahlburg, S. P. Obenschain, C. J. Pawley, V. Serlin, J. H. Gardner, Y. Aglitskiy, Y. Chan, A. V. Deniz, T. Lehecka, and M. Klapisch, Phys. Plasmas **6**, 2089 (1999).

[12] W. C. Mead and J. D. Lindl, Bull. Am. Phys. Soc. **21**, 1102 (1976).

[13] I. G. Lebo, K. Rohlena, V. B. Rozanov, V. F. Tishkin, Quantum Electronics **26**, 69 (1996); A. B. Iskakov, V. F. Tishkin, I. G. Lebo, J. Limpouch, K. Ma_ek, and K. Rohlena, Phys. Rev. E **61**, 842 (2000).

[14] E. Krousk_, O. Renner, K. Ma_ek, M. Pfeiffer, O. Pacherov , B. Kr likov , J. Sk la, and K. Rohlena, Laser and Particle Beams **18**, 87 (2000).

[15] T. J. B. Collins and S. Skupsky, Phys. Plasmas **9**, 275 (2002).

[16] J. D. Lindl and W. C. Mead, Phys. Rev. Lett. **34**, 1273 (1975).

[17] J. E. Rothenberg, Appl. Optics **39**, 6931 (2000).

[18] A. L. Velikovich, F. L. Cochran, and J. Davis, Phys. Rev. Lett. **77**, 853 (1996); A. L. Velikovich, F. L. Cochran, J. Davis, and Y. Chong, Phys. Plasmas **5**, 3377 (1998).

J. H. Hammer, J. L. Eddleman, P. Springer, M. Tabak, A. Toor, K. Wong, G. B. Zimmerman, C. Deeney, R. Humphreys, T. J. Nash, T. W. L. Sanford, R. B. Spielman and J. S. DeGroot, Phys. Plasmas **3**, 2063 (1996).

[19] Y. Song, P. Coleman, B. H. Failor, A. Fisher, R. Ingermanson, J. S. Levine, H. Sze, E. Waisman, R. J. Commisso, T. Cochran, J. Davis, B. Moosman, A. L. Velikovich, B. V. Weber, D. Bell and R. Schneider, Rev. Sci. Instrum. **71**, 3080 (2000).

[20] H. Sze, J. Banister, P. L. Coleman, B. H. Failor, A. Fisher, J. S. Levine, Y. Song, E. M. Waisman, J. P. Apruzese, R. W. Clark, J. Davis, D. Mosher, J. W. Thornhill, A. L. Velikovich, B. V. Weber, C. A. Coverdale, C. Deeney, T. Gilliland, J. McGurn, R. Spielman, K. Struve, W. Stygar, and D. Bell, Phys. Plasmas **8**7, 3135 (2001).

[21] V. N. Goncharov, Phys. Rev. Lett. **82**, 2091 (1999);

[22] A. L. Velikovich, J. P. Dahlburg, J. H. Gardner, and R. J. Taylor, Phys. Plasmas **5**, 1491 (1998); V. N. Goncharov, S. Skupsky, T. R. Boehly, J. P. Knauer, P. McKenty, V. A. Smalyuk, R. P. J. Town, O. V. Gotchev, R. Betti, and D. D. Meyerhofer, Phys. Plasmas **7**, 2062 (2000);

[23] Y. Aglitskiy, A. L. Velikovich, M. Karasik, V. Serlin, C. J. Pawley, A. J. Schmitt, S. P. Obenschain, A. N. Mostovych, J. H. Gardner, and N. Metzler, Phys. Rev. Lett. **87**, 265001 (2001).

[24] Y. Aglitskiy, A. L. Velikovich, M. Karasik, V. Serlin, C. J. Pawley, A. J. Schmitt, S. P. Obenschain, A. N. Mostovych, J. H. Gardner, and N. Metzler, Phys. Plasmas **9**, 2264 (2002).

[25] H. Nishimura, H. Shiraga, M. Nishikino, H. Azechi, N. Miyanaga, M. Nakai, K. Shigemori, Y. Ochi, K. Fujita, N. Izumi, R. Kodama, M. Matsuoka, M. Murakami, K. Nishihara, R. Ishizaki, N. Ohnishi, H. Takabe, K. Nagai, T. Norimatsu, K. Mima, and T. Yamanaka, *Inertial Fusion Science and Applications — State of the Art 1999*, Proceedings of the first international conference on Inertial Fusion Sciences and Applications, Bordeaux, France, 1999, edited by C. Labaune, W. J. Hogan and K. A. Tanaka (Elsevier, Paris, 2000), p. 148.

[26] R. H. Lehmberg and J. E. Rothenberg, J. Appl. Phys. **87**, 1012 (2000); also see EPAPS Document No. E-PHPAEN-8-992105 for Analysis of intensity structure of the ISI model in the FAST2D hydrocode by A. J. Schmitt. This document may be retrieved via the EPAPS homepage ~http://www.aip.org/pubservs/epaps.html or from ftp.aip.org in the directory/epaps/. See the EPAPS homepage for more information.

[27] S. P. Obenschain, S. E. Bodner, D. Colombant, K. Gerber, R. H. Lehmberg, E. A. McLean, A. N. Mostovych, M. S. Pronko, C. J. Pawley, A. J. Schmitt, J. D. Sethian, V. Serlin, J. A. Stamper, C. A. Sullivan, J. P. Dahlburg, J. H. Gardner, Y. Chan, A. V. Deniz, J. Hardgrove, T. Lehecka, M. Klapisch, Phys. Plasmas **3**, 2098 (1996).

[28] S. E. Bodner, D. G. Colombant, J. H. Gardner, R. H. Lehmberg, S. P. Obenschain, L. Phillips, A. J. Schmitt, J. P. Sethian, R. L. McCrory, W. Seka, C. P. Verdon, J. P. Knauer, B. B. Afeyan, and H. T. Powell, Phys. Plasmas **5**, 1901 (1998).

[29] Ya. B. Zel dovich and Yu. P. Raizer*, Physics of Shock Waves and High-Temperature Hydrodynamic Phenomena* (Dover Publications, New York, 2002), Chapter XII.

[30] W. H fele, Z. Naturforsch. **10a**, 1006 (1955); V. B. Adamskii, Sov. Phys. Acoust. **2**, 1 (1956); Ya. B. Zel dovich, Sov. Phys. Acoust. **2**, 25 (1956); A. I. Zhukov and Ya. M. Kazhdan, Sov. Phys. Acoust. **2**, 375 (1956).

[31] L. I. Sedov, *Methods of Similarity and Dimensional Analysis in Mechanics*, 10th ed. (CFC Press, Boca Raton, 1993).

[32] J. P. Boris and D. L. Book, J. Comput. Phys. **11**, 38 (1973), also see Solution of the Continuity Equation by the Method of Flux-Corrected Transport, *Methods in Computational Physics*, v. 16 (Academic Press, New York, 1976), pp. 85-129.

[33] A. L. Velikovich, A. J. Schmitt, J. H. Gardner, and N. Metzler, Phys. Plasmas **8**, 592 (2001).

[34] J. Meyer-ter-Vehn, Plasma Phys. Contr. Fusion **43**, Suppl. 12A, A113 (2001).

Figure captions

Fig. 1. Time evolution of the density profiles in a foam-plastic sandwich target irradiated by a 0.325 ns long shaping pulse at t = -12 ns. The profiles are shown with a 1 ns interval.

Fig. 2. Time evolution of the density profiles (a) and the x-t diagram showing shock dynamics (b) for the same conditions as in Fig. 1 but with the drive laser pulse following the shaping pulse. The upper envelope curve of the high-density area is the ablation front. When the shaping pulse is applied, this curve is concave at early time, which implies deceleration.[3]

Fig. 3. (a) Shape of the standard Nike pulse with a low-intensity foot (solid line) and without a foot (dashed line, shifted by ~0.5 ns closer to the shaping pulse, to provide matching under the conditions of Fig. 1). t = 0 is the moment when the Nike pulse with a foot reaches half-maximum. The shaping pulse starts at t = -12 ns. (b) The x-t diagram showing shock dynamics for a 62 μm solid plastic target irradiated with a Nike pulse and no shaping pulse. In this case the ablation front is never concave.

Fig. 4. (a) Evolution of mass variation amplitude in a sandwich target with and without the 0.325 ns shaping pulse (the single-mode, constant phase intensity variation is the same in the shaping pulse and the drive pulse) and in a solid plastic target without a shaping pulse. (b) Same comparing the effects of a 0.325 ns, 1.3 ns and 0.1 ns shaping pulses with a 2% intensity modulation in a sandwich target. All the other simulations in this paper utilized the 0.325 ns shaping pulse.

Fig. 5. Evolution of mass variation amplitude in a sandwich target rippled from the surface with and without the 0.325 ns shaping pulse; both the shaping pulse and the drive

pulse are perfectly uniform. The shaping pulse is seen to produce strong sonic oscillations whose amplitude exceeds the initial mass variation due to the surface ripples.

Fig. 6. Evolution of mass variation amplitude in a sandwich target with both shaping and drive laser pulses ISI smoothed at 1 THz bandwidth. (a) The shaping pulse is a single beam, the drive pulse is 36 overlapping beams. (b) Both the shaping and the drive pulses are 36 overlapping beams. (c) No shaping pulse.

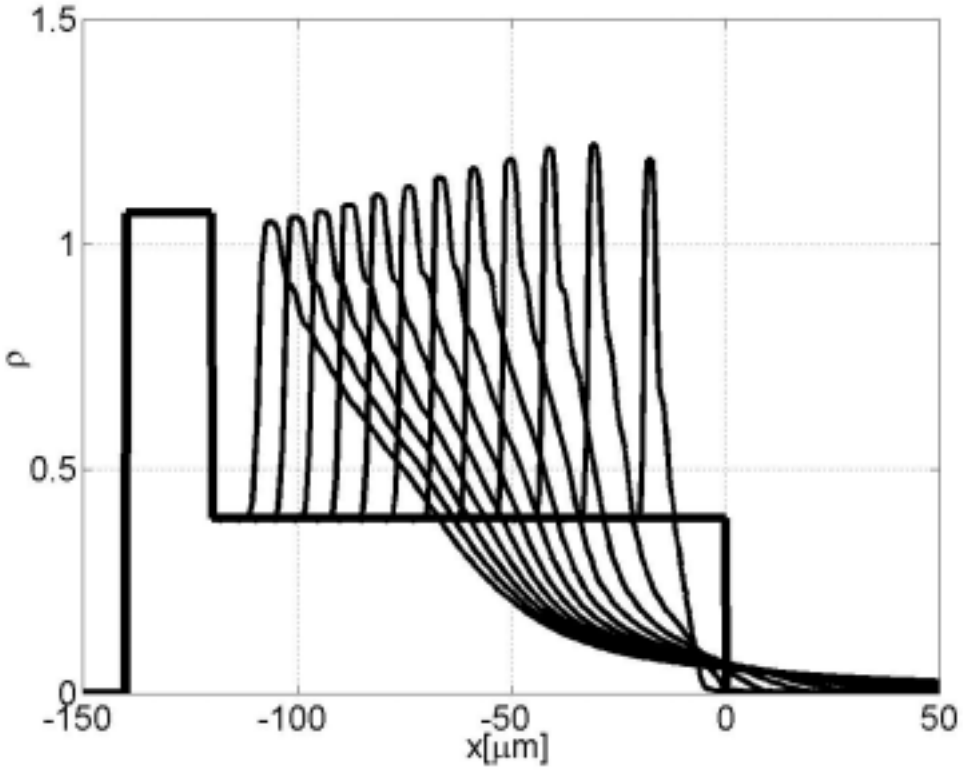

Fig. 1.

Metzler *et al*., Fig. 1

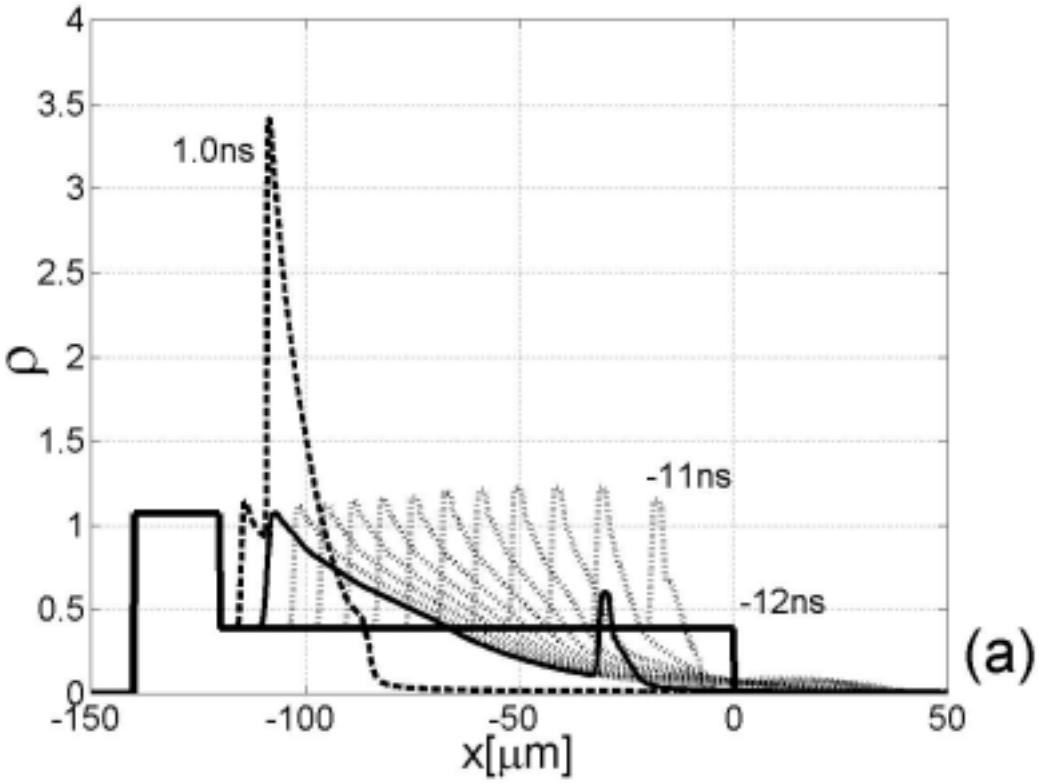

Fig. 2(a).

Metzler *et al*., Fig. 2(a)

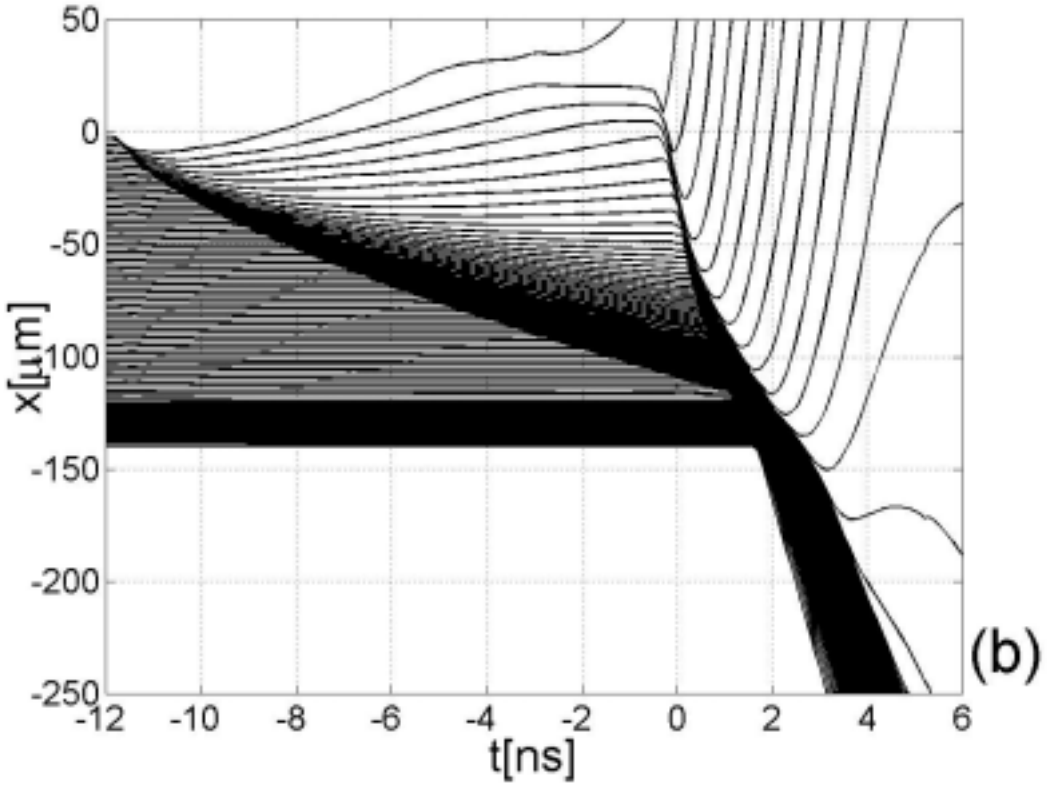

Fig. 2(b).

Metzler *et al*., Fig. 2(b)

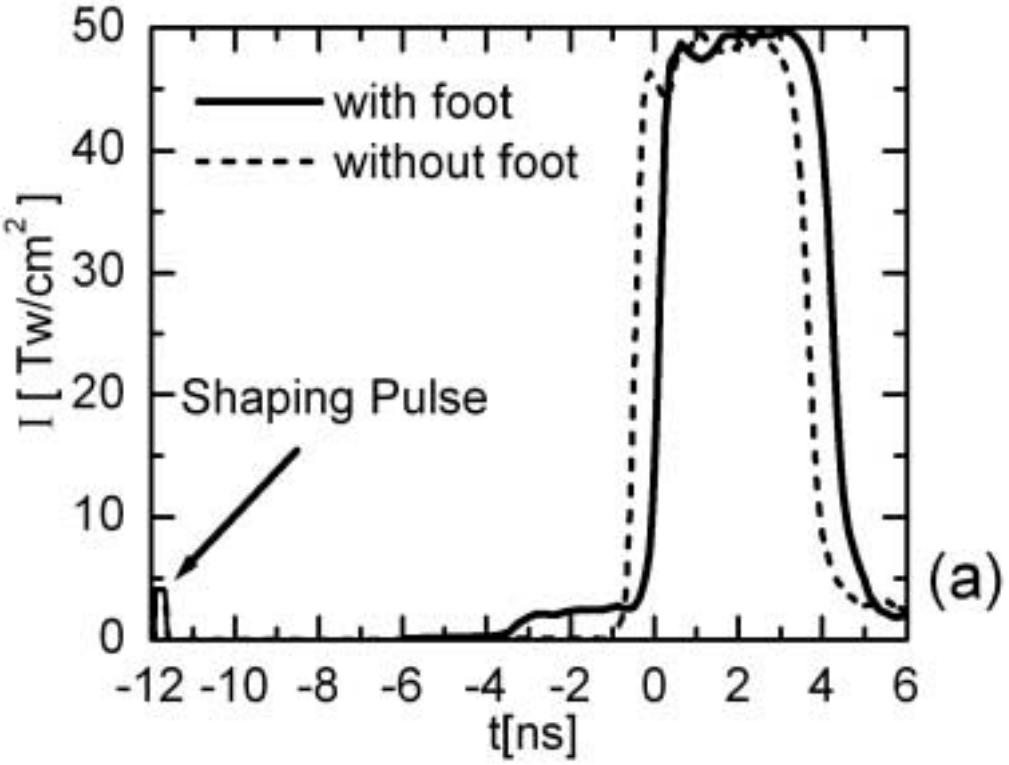

Fig. 3(a).

Metzler *et al*., Fig. 3(a)

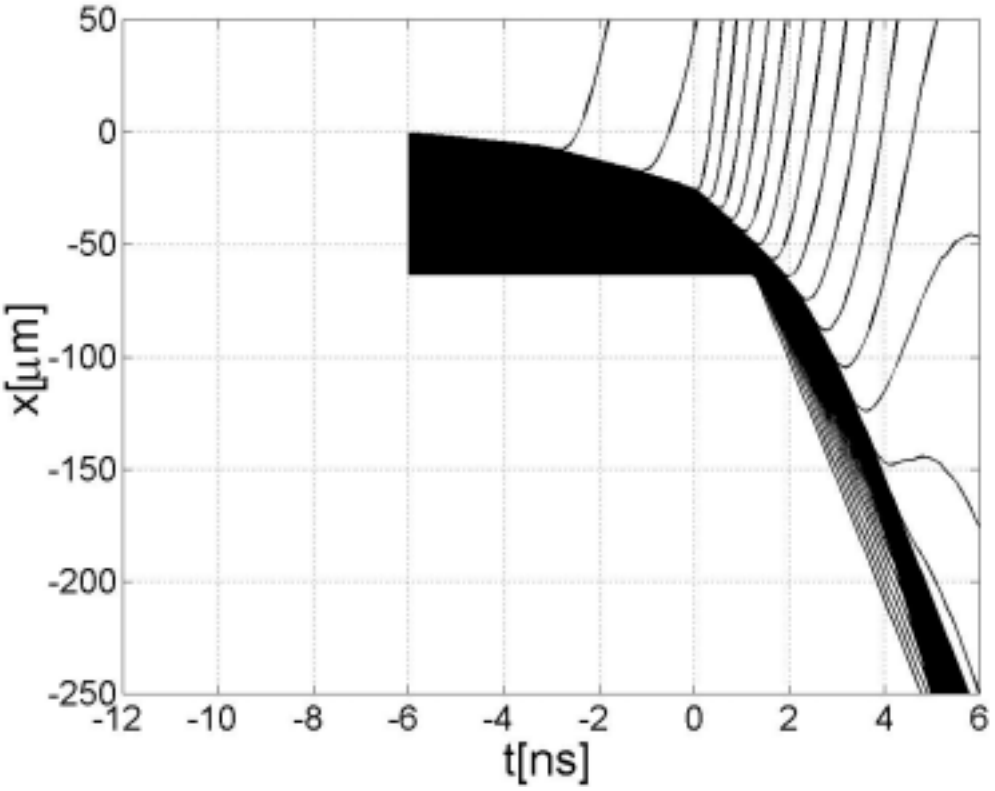

Fig. 3(b).

Metzler *et al*., Fig. 3(b)

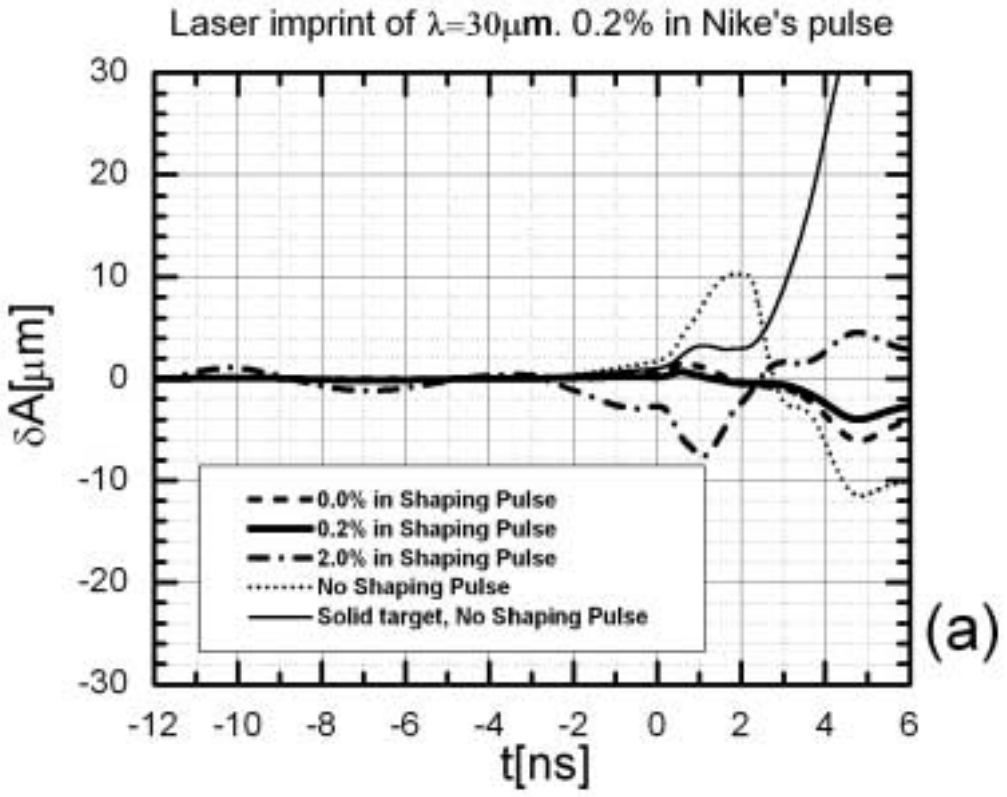

Fig. 4(a).

Metzler *et al*., Fig. 4(a)

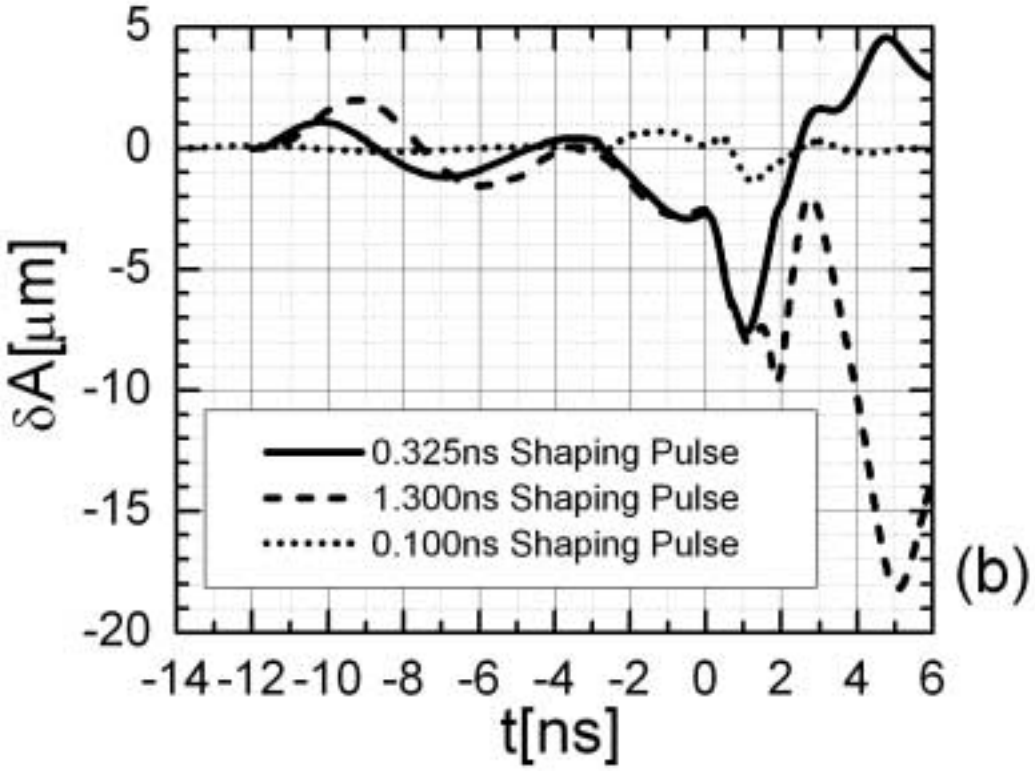

Fig. 4(b).

Metzler *et al*., Fig. 4(b)

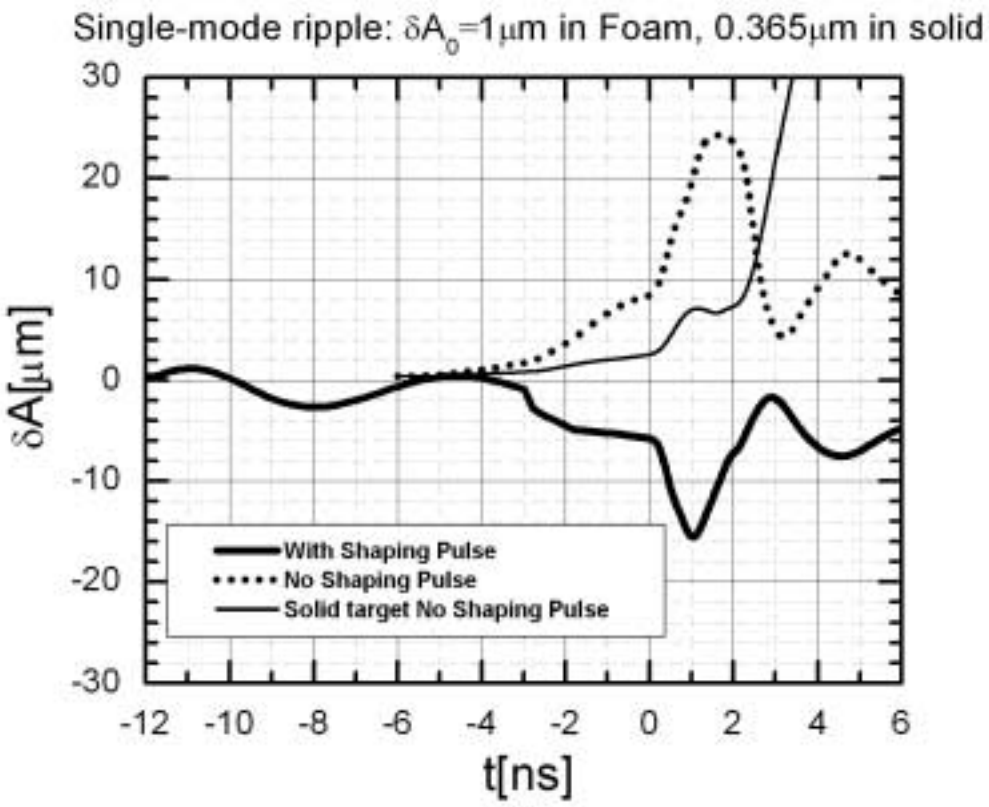

Fig. 5.

Metzler *et al*., Fig. 5

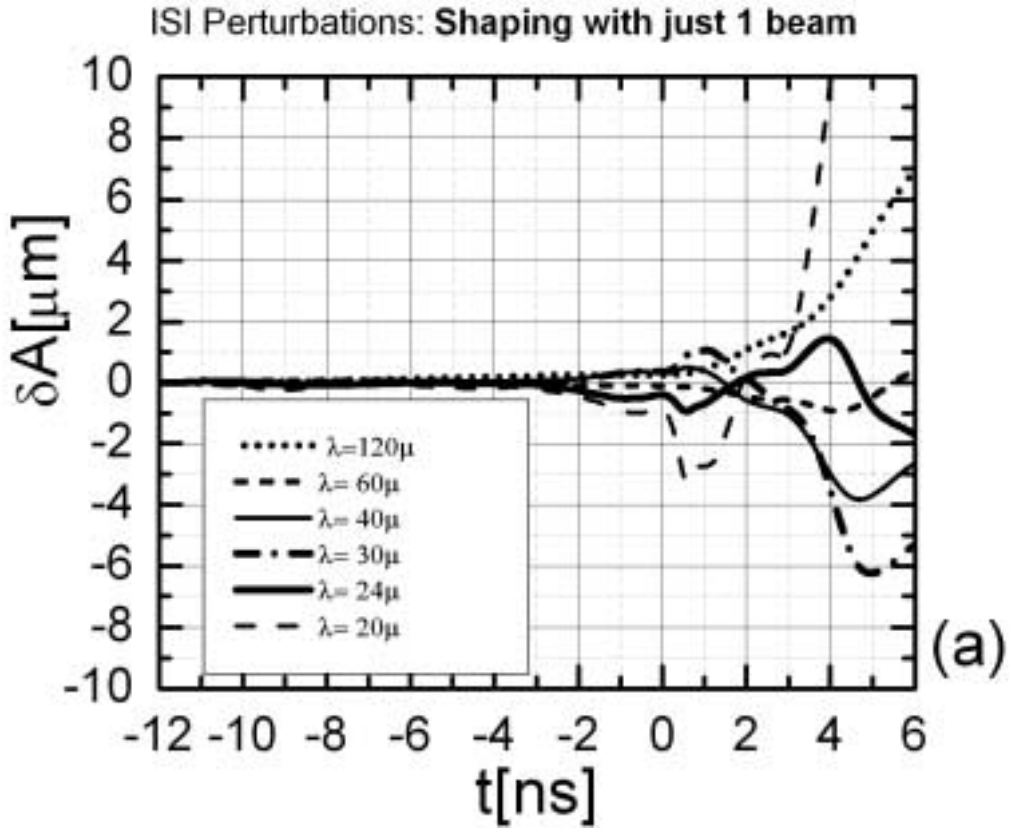

Fig. 6(a).

Metzler *et al*., Fig. 6(a)

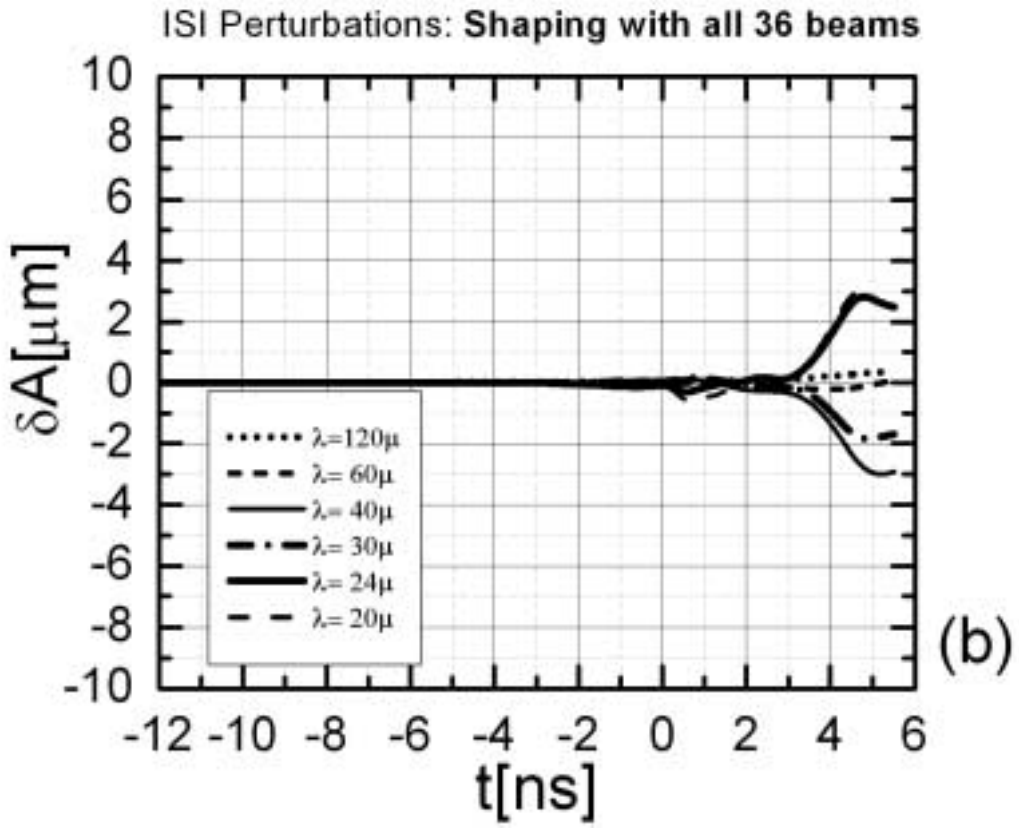

Fig. 6(b).

Metzler *et al*., Fig. 6(b)

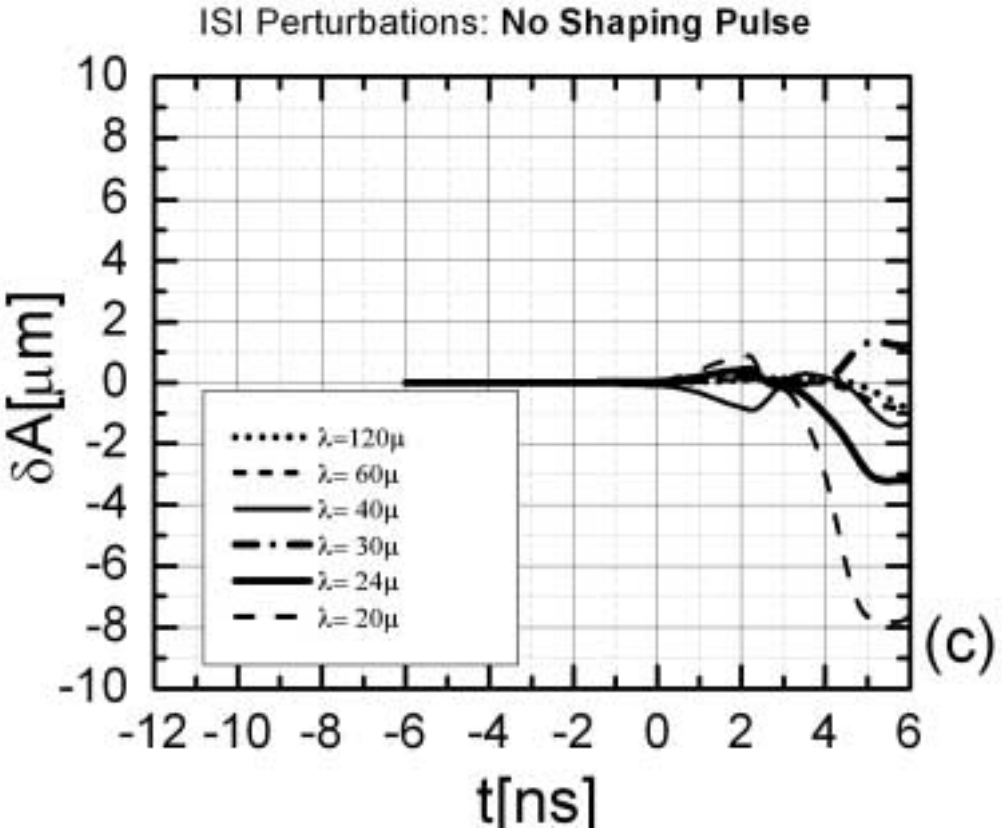

Fig. 6(c).

Metzler *et al*., Fig. 6(c)